

Kinetic damage analysis of composite carbon fiber/epoxy

FACI Youcef¹, A.Mebtouche², B.Berdjene³, B.Maalem⁴, H.dehdouh⁵

¹ Bp 64, route dely brahim Cheraga, Algiers, ALGERIA

Email: y.faci@crti.dz

Abstract

Fiber reinforced composite materials have been increasingly used as structural material in airplanes and in space applications because of their high specific stiffness and strength. This work presents the results of the damage kinetic of carbon fiber reinforced polymer using the acoustic emission under solicitations. The correlations between acoustic emission parameters and damage mechanism are identified, and then confirmed by microscopic observations. This review will emphasize the roles that AE can play as a tool for the composite materials, damage mechanisms, and characterization of damage evolution with increasing time or stress, the localization and origin of damage, quantification of crack size based on energy release from concrete structures in the field and reduction in the numbers of test specimens required in various studies.

Keys: *kinetic, damage, simulation, energy, acoustic emission.*

Introduction

The formation and propagation of cracks in composite is a field of research that has been active for decades. The theoretical description of the physics at the crack dynamics are active fields of research [1-2]. A phenomenon that is closely related to the crack dynamics is the generation of acoustic waves due to the crack motion due to the release of stored elastic energy. These acoustic waves propagate within the solid and can be detected at the surface by suitable sensor systems. A small amount of work has been performed recently to advance the understanding of the physical processes involved in the generation of acoustic emission.

Meanwhile, various valuable attempts have been made to provide a theoretical description of acoustic emission sources. Here, source models are geometrically approximated as point sources, while the dynamic of the source is either approximated from iterative refinement of model parameters to fit experimental data or is based on assumptions on the source dynamics derived from structural mechanics. Various step-function descriptions exist, which are used to describe the three dimensional spatial displacement of the crack surface during crack formation [3-4]. In particular, the rise-time of the initial crack surface displacement is an essential parameter to model the crack surface motion [5]. However, there are no reports in literature of successful measurements of rise-times of real acoustic emission sources, e.g. due to crack formation in materials. Instead the rise-time is typically estimated based on the elastic properties of the bulk material. This type of source modeling has been successfully applied to many cases, and the basic concept has been used within the generalized theory of acoustic emission by Ono and Ohtsu [6]. In recent years it has become convenient to use numerical methods to model acoustic emission sources. In this field, Prosser, Hamstad and Gary applied finite element modeling to simulate acoustic emission sources based on body forces acting as a point source in a solid [6, 7]. Hora and Cervena investigated the difference between nodal sources, line sources and cylindrical sources to build geometrically more representative acoustic emission sources [8]. At the same time, we proposed a finite element approach using an acoustic emission source model taking into account the geometry of a crack and the inhomogeneous elastic properties in the vicinity of the acoustic emission source.

Experimental Procedure

The investigation studying the relationships between AE energy and fracture area and depth was applied to the practical AE waveforms recorded during the instantaneous failure of a composite specimen of known fracture area and depth. The mix proportions of the concrete beams was arranged so that the mass ratios of the specimen. The first specimen had dimensions 3.4 mm width, 35, 2 mm depth and 134.4 mm length. The second specimen had of 2.4 mm width, 34.2mm depth and a length of 134.2mm. The third one had of 1.4 mm width, 34.2mm depth and a length of 134.2mm.

Fifteen specimens were created with a constant crack depth but a varying crack area and fourteen specimens were created with a constant crack area but a varying crack depth. Table 1 shows the dimensions of all the notched areas. The mortar specimens were grouted into the concrete beam and failed by an instantaneous force supplied by a kilogram weight dropped at a height of 1m from the specimen. Rubber was attached to both the specimen and the drop weight to prevent any crushing during testing. A diagram of the test set-up including the loading method can be seen in Fig. 1.

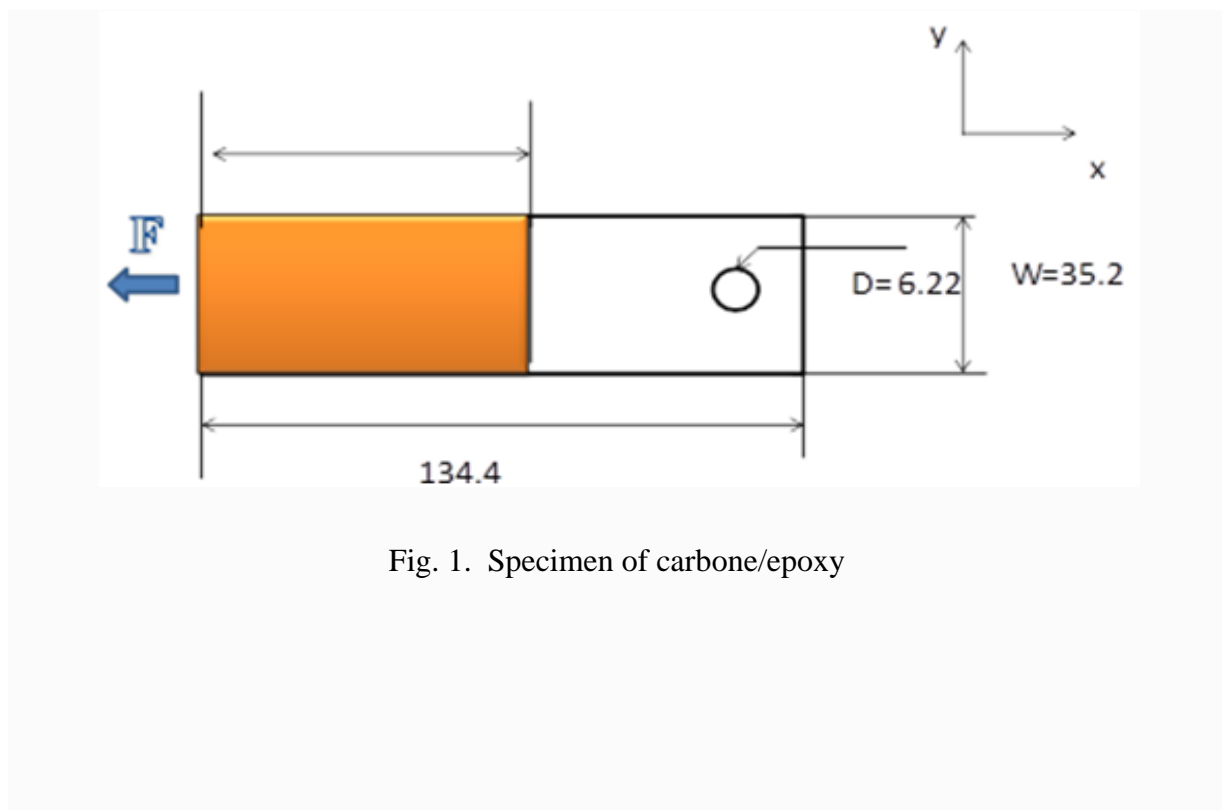


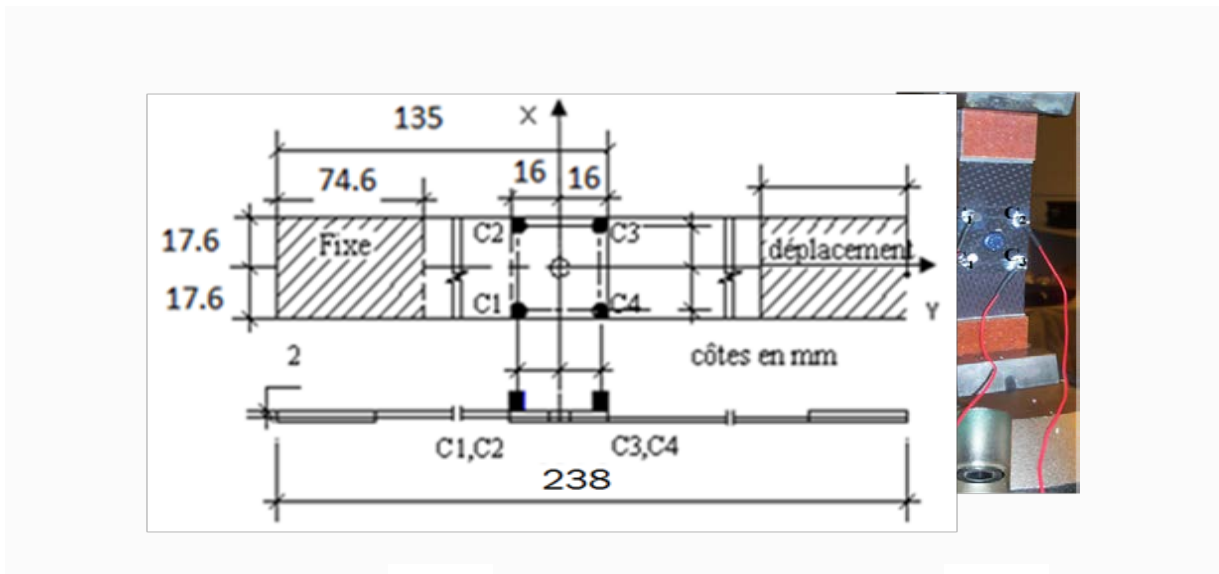
Fig. 1. Specimen of carbone/epoxy

Notch area (depth mm*with mm)	Area (mm ²)
34,2*3,4	116,28
34,2*2,5	85,5
34,2*1,4	47,88

Table1: Dimension of specimens

Instrumentation

Four AE sensors were attached to the concrete beams to detect AE waveforms produced during the failure of the substrate until failure. The sensors had a resonant frequency of 1 kHz, to 1 MHz and were pre-amplified by 40dB. A threshold of 50dB was used so that only large concrete cracks were monitored. AE waveforms detected at the sensors were recorded by a digital memory, which converted analogue records into digital records at a sampling rate of 1MHz. The frequency detection range employed was 10kHz-1MHz. The sensor positioning and location can also be seen in Fig. 2.



(1) (2)
 Figure 02: Localization of sensors C₁, C₂, C₃, and C₄

Results and Discussion

When analyzing the data it is important that the correct events are chosen. A waveform from a typical fracture is shown in Fig. 3 together with event based display. From this information the absolute energy recorded on each sensor during the fracture of the assembly specimen can be found. By highlighting a certain AE event all the parameters can be extracted. In this case the fracture is represented by the event with the largest amplitude as shown by the plot in the top wright's corner of Figure. 3. As well as amplitude versus time, the amount of energy recorded during the failure can be seen. Fig. 3

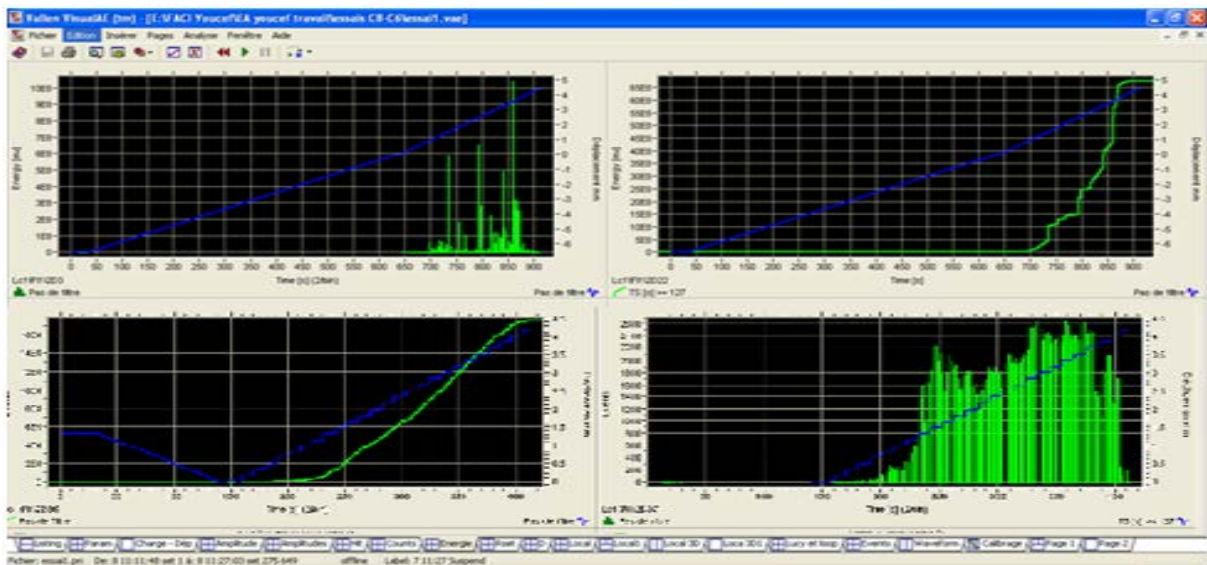


Figure 03: Energy parameters from a typical specimen fracture (116.28 mm² Area).

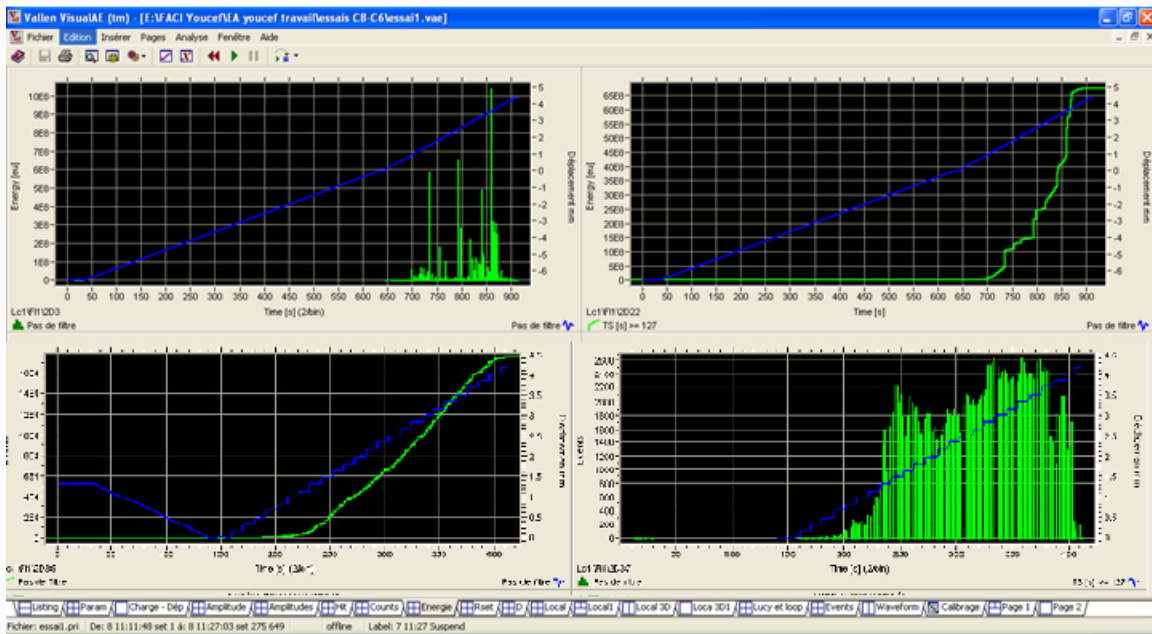


Figure 04 Energy parameters from a typical specimen fracture (85,5 mm² Area).

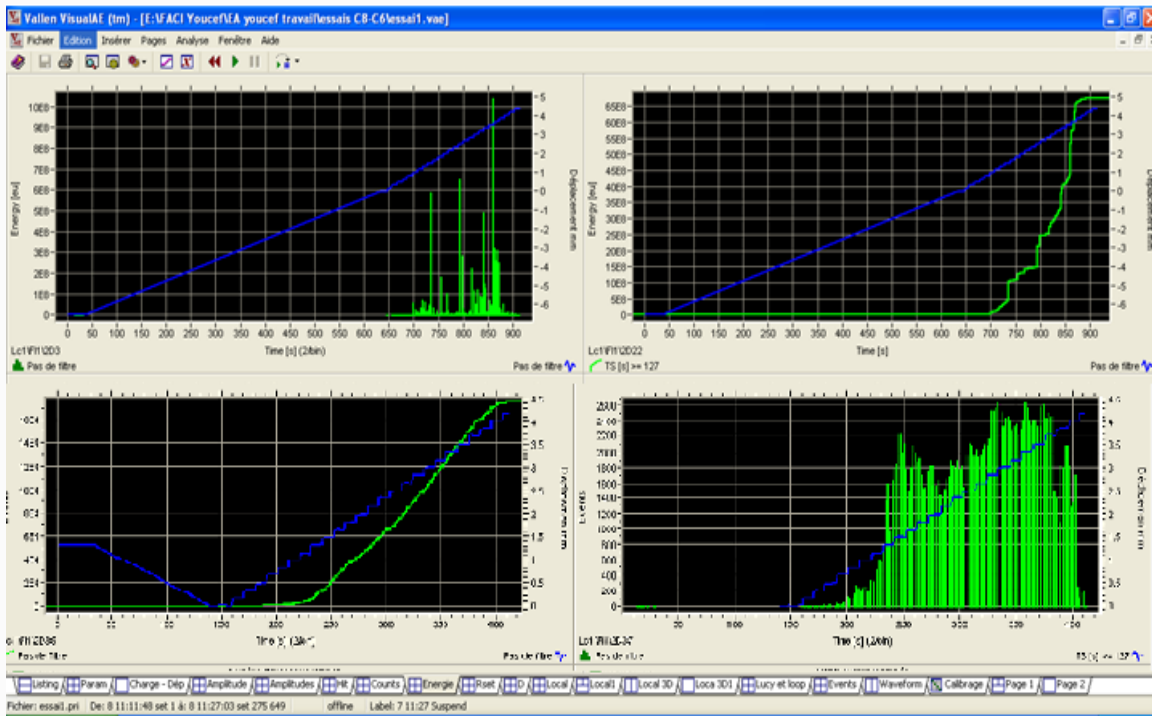


Figure 05: Energy parameter from a typical specimen fracture (47,88 mm² Area).

6th International Conference on Green Energy and Environmental Engineering GEEE-2019

As mentioned previously the amount of AE energy recorded during the failure is expected to be related to the size of the crack in some way. Figs. 4 and 5 show the amount of energy recorded on the frequency sensor for specimens with varying crack depths. These graphs show that even though the crack area is constant the amount of energy increases with crack depth. Fig. 5 represents similar data to that of Fig. 4 and 3 but shows how the energy varies with crack depth for all three of the sensors. Again even though the crack area is a constant 500mm² the energy increases with crack depth on all channels. Since high frequencies attenuate quickly in concrete, the sensors with lower resonant frequency record higher amounts of energy.

Conclusions

In this paper a study was performed to correlate AE energy produced during the failure of specimen to either crack area or crack depth. It was found that the amount of AE energy produced by the failure of the specimens could be related to crack depth. It is hoped that these results and results from further testing can be used to aid the quantification of crack size based on energy release from concrete structures in the field.

References

- [1].Livne, A., Bouchbinder, E., Fineberg, J.: Breakdown of linear elastic fracture mechanics near the tip of a rapid crack. *Phys. Rev. Lett.* **101**, 264–301 (2008) [CrossRef](#) [Google Scholar](#)
- [2].Livne, A., Bouchbinder, E., Svetlizky, I., Fineberg, J.: The near-tip fields of fast cracks. *Science* **327**, 1359–1363 (2010) [CrossRef](#) [MATHMathSciNet](#) [Google Scholar](#)
- [3].Buehler, M., Gao, H.: Dynamical fracture instabilities due to local hyperelasticity at crack tips. *Nature* **439**, 307–310 (2006) [CrossRef](#)[Google Scholar](#)
- [4].Fineberg, J., Gross, S.P., Marder, M., Swinney, H.L.: Instability in dynamic fracture. *Phys. Rev. Lett.* **67**, 457–460 (1991) [CrossRef](#)[Google Scholar](#)
- [5].Hamstad, M.: On lamb modes as a function of acoustic emission source rise time. *J. Acoust. Emiss.* **27**, 114–136 (2009) [Google Scholar](#)
- [6].Ohtsu, M., Ono, K.: A generalized theory of acoustic emission and Green's function in a half space. *J. Acoust. Emiss.* **3**, 27–40 (1984) [Google Scholar](#)
- [7].Prosser, W., Hamstad, M., Gary, J., O'Gallagher, A.: Comparison of finite element and plate theory methods for modeling acoustic emission waveforms. *J. Nondestruct. Eval.* **18**(3), 83–90 (1999) [CrossRef](#)[Google Scholar](#)
- [8].Hora, P., Cervena, O.: Acoustic emission source modeling. *Appl. Comput. Mech.* **4**, 25–36 (2010) [Google Scholar](#)

